# Fatigue Crack Branching Behavior in Dual Phase Material

Guocai Chai[1], Ru Lin Peng[2], Karel Slamecka[3] and Sten Johansson[2]

[1]Sandvik Materials Technology, R&D center, 811 81 Sandviken, Sweden;
[2]Linköping University, Department of Mechanical Engineering, SE 581 83 Linköping, Sweden;
[3]Brno University of Technology, Czech Republic

12th International Conference on Fracture
12–17 July, 2009
Otawa, Canada

# Fatigue Crack Branching Behavior in Dual Phase Material

Guocai Chai[1], Ru Lin Peng[2], Karel Slamecka[3] and Sten Johansson[2]
[1]Sandvik Materials Technology, R&D center, 811 81 Sandviken, Sweden; [2]Linköping University, Department of Mechanical Engineering, SE 581 83 Linköping, Sweden; [3]Brno University of Technology, Czech Republic

**Abstract.**
Fatigue crack branching behaviour in a dual phase steel has been investigated using an in-situ SEM/EBSD fatigue test and a conventional da/dN test. Crack branching results mainly from the extrusions and intrusions of slip bands developed in the grains. The number of crack branches formed depends strongly on the loading condition and the microstructure of the material. The in-situ observation confirms that the formation of crack branches can significantly reduce the crack propagation rate that leads to crack growth retardation in the main mode I crack path. The crack branches formed are usually not ideal. They can propagate almost transversely to the main crack direction with a mode II stress intensity factor, SIF, and a rate that is much higher than that of the main crack.

## 1. Introduction

It is known that fatigue cracking can significantly deviate from the propagation directions that should be perpendicular to the main stresses in mode I. This may lead to the formation of crack deflection, kinking or branching [1, 2], and consequently cause significant retardation or even arrest of the subsequent crack propagation by reducing crack driving force [2, 3].

Although it is very difficult to analyse propagation behaviour of branched cracks, several analytical solutions have been developed to predict the propagation path of a branched crack and to calculate the mode I and II stress intensity factors. They confirm that the formation of fatigue crack branches reduce the stress intensity factors and therefore the crack propagation rate [3, 4]. They also predict that a shorter branch will arrest and a longer branch will return to the pre-overload propagation [3]. These discussions were mainly focused on the overloading conditions. Most direct observations of fatigue crack branching behaviour have been made using light optical microscopes (LOM) or scanning electron microscopes (SEM). Recently, several in-situ SEM and atomic force microscope (AFM) studies on the fatigue branching behaviour have been performed [5, 6]. In these researches, fatigue crack branching behaviour and subsequent fatigue crack retardation were observed [5]. With in-situ AFM, the microscopic crack branching behaviour can be investigated [6]. However, these studies can not identify the slip systems that initiate crack branching. No information on the influence of stress intensity factor, SIF, on the fatigue crack branching behaviour has been reported.

Modern dual phase or multi phase alloys display remarkable fatigue properties. The fatigue threshold values of ferritic-martensitic duplex steels can range up to 20 MPa.m$^{1/2}$ [7]. The high threshold values of multi phase alloys are considered to be attributed to crack deflection and branching, which cause unusually high crack propagation resistance [7, 8]. In the present study, the fatigue crack branching behaviour in an austenitic-ferritic duplex stainless steel will be investigated using a newly developed in-situ SEM/EBSD fatigue tester and a conventional da/dN test. The influence of stress intensity factor and crack branching mechanism will be focused. The slip systems for crack branching will be identified.

## 2. Experimental procedure

The material used was a hot rolled bar made of austenitic ferritic duplex stainless steel SAF 2507 (equivalent to UNS S32750) with a diameter of 80 mm (AD) and a nominal chemical composition (in wt%): 0.03% C, 80% Si, 1.2% Mn, 25% Cr, 7% Ni, 4% Mo, 0,3%N and Fe. The tensile properties in the rolling direction are shown in Table 1.

Table 1 Tensile properties of SAF 2507 bar material in rolling direction

| Temperature [°C] | $\sigma_{YS}$ [MPa] | $\sigma_{TS}$ [MPa] | Elongation [%] |
|---|---|---|---|
| 20 | 625 | 820 | 41.7 |

Fatigue crack growth (FCG) rate test was performed using 18 mm thick compact C(T) specimens with TS orientation in an MTS servo-hydraulic machine (50kN). The main tests were performed using K-gradient constant value of $Cg$=-0.1 mm$^{-1}$ in air at RT. The mean stress ratio R is 0.1 and the frequency is 10 Hz. The fatigue crack paths and mechanisms were investigated using SEM and LOM. Evaluation of fatigue crack branching was done by analyzing high-resolution bitmap images acquired at magnification 1000× by means of the LOM. The number of short branches together with the origin of their initiation (within the ferritic grain, within the austenitic grain, at the ferrite-austenite grain boundary) was assessed.

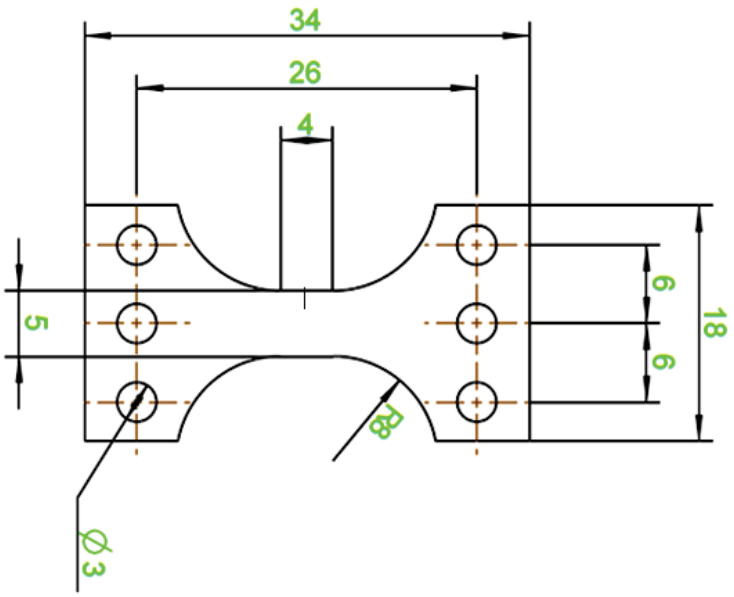


Fig. 1 The geometry of the tensile specimen for in-situ SEM/EBSD examination.

For in-situ SEM/EBSD experiments, a small specimen with a thickness of 1.513 mm and width of 5 mm was machined from a bending fatigue pre-cracked specimen with the crack at the mid-length of the gauge section. The geometry of the specimen is shown in Fig. 1. The length of the crack is 1.18 mm. The specimen was mounted on a Gatan microtester which was then inserted into the sample chamber of a Hitachi SU-70 scanning electron microscope. With the build-in pre-tilting fixture the carefully prepared surface of the specimen was in $20^{o}$ tilt with respect to the incident electron beam. The EBSD detector and Channel 5 software from the Oxford Instrument were used for the in-situ EBSP mapping.

Tests with a peak load varying from 1800 N to 2800 N was carried out first to find a suitable growth rate which allows the in-situ experiment to be performed within a reasonable time frame. Finally, a cyclic load between 2800 and 280 N (R=0.1) was induced with a frequency of 0.0125Hz. The fatigue test was stopped after loading to different number of cycles for imaging by SEM or EBSP.

### 3. Results and discussion

Table 2 shows a summary of the testing results from the conventional da/dN test. The Paris law constants, $C_m$ and n, were evaluated. $\Delta K_{cl,th}$ and $\Delta K_{eff,th,}$ are also compared. The results show that this material has a very high closure threshold, $\Delta K_{cl,th}$, which is even higher than the effective thresholds, $\Delta K_{eff,th}$. The thresholds evaluated by analyzing the load versus crack opening displacement (COD) curves (sum of $\Delta K_{cl,th}$ and $\Delta K_{eff,th,}$) are comparable to those determined from the da/dN versus $\Delta K$ curves, $\Delta K_{th,exp}$.

Table 2 Paris law's constants and threshold values

| $C_m$ (mm/cycle) | n | $\Delta K_{th,exp}$ (MPa√m) | $\Delta K_{cl,th}$ (MPa√m) | $\Delta K_{eff,th}$ (MPa√m) | $\Delta K_{cl,th} + \Delta K_{eff,th}$ (MPa√m) |
|---|---|---|---|---|---|
| $5.35 \times 10^{-10}$ | 3.52 | 8.64 | 5,35 | 3,90 | 9,25 |

Fig. 2 shows the fatigue cracking path in SAF 2507 bar material at RT. The arrows indicate where a crack branching appears. It can be seen that the crack path is not straight and consists of numbers of crack deflections and crack branches. Fatigue crack branching can occur in both ferritic and austenitic phases, but can also be observed at phase boundaries. Most of the branches are not ideal. The angle between two branches (2θ) varies greatly. Some of them are close to 180°. There are mainly two types of branching events: (i) 'short branches' with the length l≤15μm and (ii) long branches with the length l>30μm. Only a few cracks ceased to grow at an intermediate length 15μm≤ l ≤30μm.

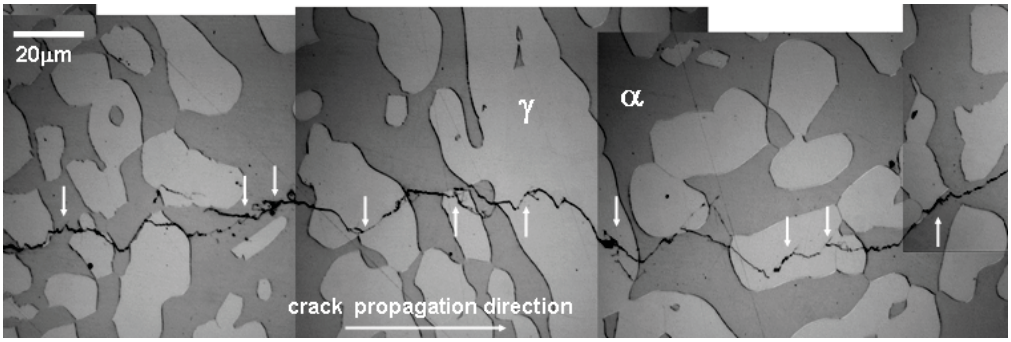


Fig. 2 Fatigue crack path in SAF 2507 bar material from a conventional fatigue propagation test. The arrows indicate where a crack branching appears. γ is the austenitic phase and α is the ferritic phase.

It was observed that the occurrence of fatigue crack branching depends on the loading condition and the microstructure of the material. As shown in Fig. 3, the number of crack branches increase with increasing applied stress intensity factor range $\Delta K$. Near the fatigue crack threshold regime, the probability for the formation of fatigue crack branch has greatly reduced. The result also shows that fatigue crack branching occurs mainly inside grains, and the number of crack branches seems also higher in the austenitic phase than in the ferritic phase. This may be due to the fact of the heterogeneous plastic deformation in this alloy [9]. The cyclic plastic deformation occurs first in the austentic phase since it is the soft phase in the beginning [9]. This indicates that the formation of fatigue crack branches results from the cyclic damage due to the formation of slip bands, which was also confirmed by reference [6] and the present EBSD work. The constraint of slip deformation due to the cyclic strain hardening is mainly responsible for crack branching [6].

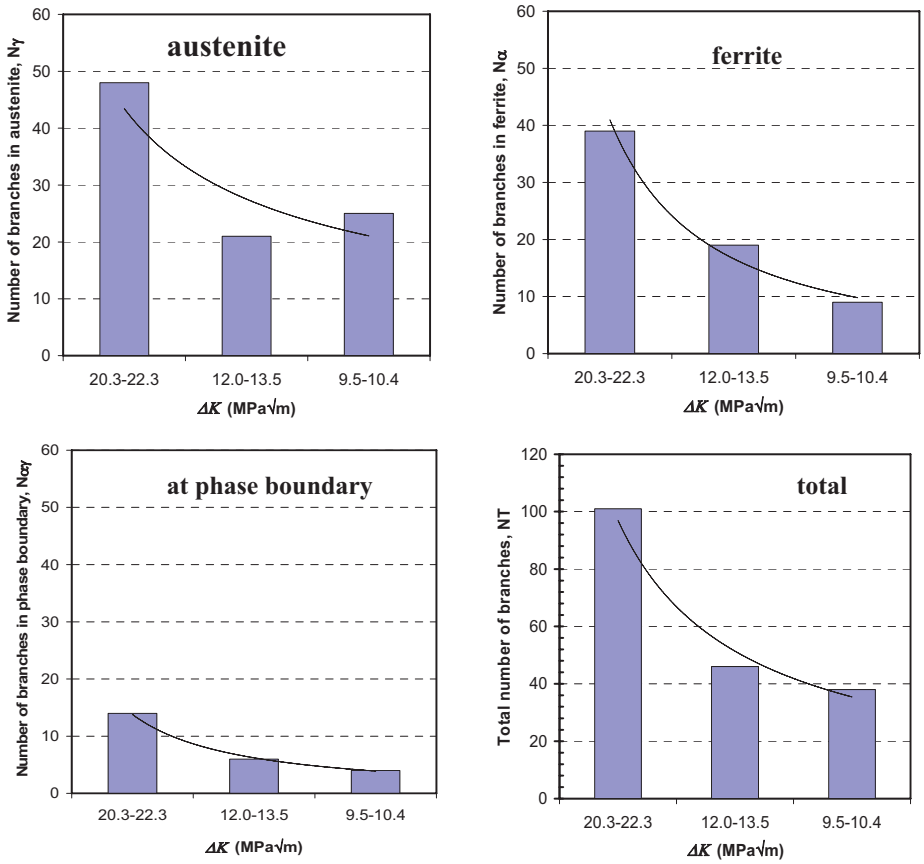


Fig. 3 Influence of load condition and microstructure on the formation of fatigue crack branching.

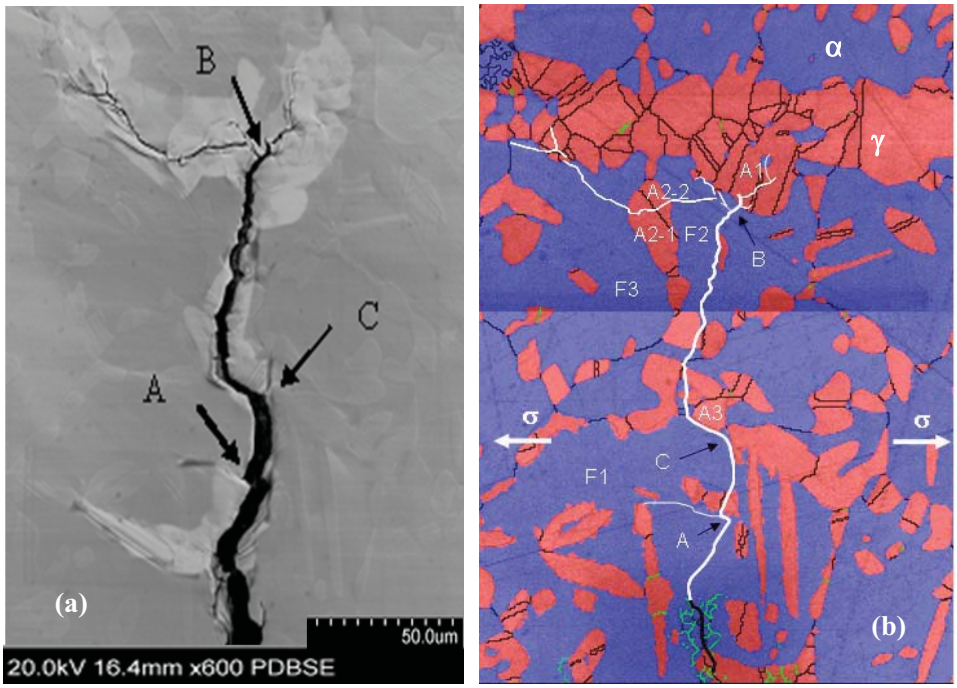


Fig. 4 (a). Backscatter electron image taken after the in-situ fatigue test was terminated and unloaded; (b). EBSD image with crack growth path indicated by thick white line (the main crack) and thin white lines (branches). The dark line is the pre-fatigue cracking. The loading direction is horizontal.

The in-situ fatigue test was terminated after reaching 5100 cycle. The specimen was unloaded and the surface was cleaned with replica and acetone. Fig. 4a is a backscatter electron image, which reveals the crack geometry. Both crack deflection and branching are obvious. The first one appears at about 500 cycles (A) and the second one at about 3800 cycles (B), while the significant deflection is marked by 980 cycles (C). Fig. 4b is an EBSD image of the region taken before the fatigue crack passed through, in which the microstructure of the duplex stainless steel is shown. The high angle grain boundaries, plotted in thin black lines, are defined as larger than 10 degrees. A microstructure with fine austenitic grains (red) distributed in a matrix of relatively large ferritic grains (blue) is clearly shown. Furthermore, the distribution of austenite is not homogenous. In certain regions, bands containing mainly austenitic grains are observed.

Table 3 Active slip systems in the ferritic phase

| Grain number | [uvw]//LD | Slip system | Schmidt's factor | Slip trace to LD |
|---|---|---|---|---|
| F1 | 1-10 | (-112)[1-11] | 0.47 | 49°/131° |
| | | (1-12)[-111] | 0.47 | 130°/50° |
| F3 | 22-1 | (11-2)[111] | 0.46 | 98°/82° |
| | | (01-1)[111] | 0.41 | 128°/52° |

LD: Loading direction

The fatigue crack path is also shown in Fig. 4b. The main crack, marked with thick white line, grew from the pre-cracking (thick black line). Obviously, the

observed branching and deflection behavior is dependent on the microstructure. Within the ferritic grains, the crack propagates in a transgranular manner. In the austenitic grains both intergranular and transgranular cracking is observed. A local change of the microstructure, namely the existence of a austenite dominant region in the front of the crack tip causes a large deflection, see for example C in Fig. 5a, or branching (A and B). A closer observation reveals extensive plastic deformation and dense slip lines around the crack tip. Table 3 shows the slipping behavior observed near the transgranular cracking in the ferrite during the in-situ test. Slip on multiple systems is dominant. For example, in the F1 grain two groups of slip bands, determined from the EBSD data to form on the (-112)[1-11] and (1-12)[-111] system (Table 3), respectively, are observed at the crack tip. Both slip systems have a comparable Schmidt's factor of 0.47 but operate in different directions.

The main crack length is plotted as a function of the number of loading cycles in Fig. 5a. The average crack propagation rates between two measure points are shown in Fig. 5b. As can be seen the crack growth rate changes at 500 cycles or 3800 cycles (regions A or B) and becomes lower (Fig. 5b). This can correlate to the formation of crack branching. The formation of crack branches will reduce the mode I crack driving force, which leads to a crack growth retardation for the main crack path [2-4]. On the other hand, some crack branches propagate almost transversely to the main crack direction with a mode II SIF. In the beginning, they propagate with a rate that is much higher than that of the main crack (Fig. 5b), and then the growth will stop somewhere in spite of that its length is longer than that in the main crack path. This contradicts to the result from the analytical solution [4].

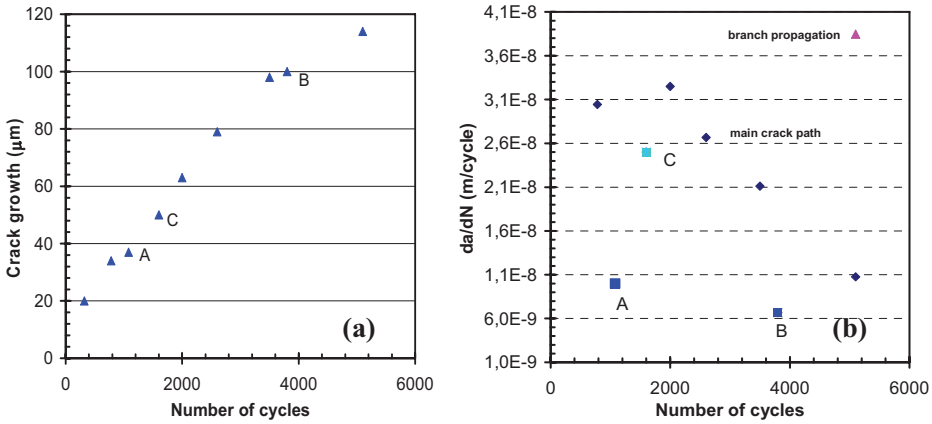


Fig. 5 (a). Crack length versus number of loading cycles; (b). Average crack growth rate versus number of loading cycles, average crack propagation rate was calculated as the ratio of the corresponding loading cycles.

## 4. Concluding remarks

Crack branching is an important crack propagation behavior in a duplex stainless steel SAF 2507. Crack crack branching occurs mainly in the grains due to the intrusion and extrusion of the slip bands. The number of crack branches formed depends on the loading condition and the microstructure of the material.

In-situ observation confirms that the formation of crack branches can significantly reduce crack propagation rate that leads to crack growth retardation in the main crack path. The crack branches formed are usually not ideal. They can propagate almost transverse to the main crack direction with a mode II SIF and a rate that is much higher than that of the main crack.

The branching behavior in the material leads to a high fatigue threshold value since they have caused high crack growth retardation and high crack closure.


## Acknowledgment

This paper is published by permission of Sandvik Materials Technology. The support of Mr M. Lundström is gratefully acknowledged.


## References


[1] J. Lankford and D.L. Davidson: Advances in Fracture Research, Vol. 2 (1981), p. 899.

[2] S. Suresh: Engrg Fracture Mechanics, Vol. 18 (1983), p. 577.

[3] M.A. Meggiolaro, A.C.O. Miranda, J.T.P. Castro, L.F. Martha: International Journal of Fatigue Vol. 27 (2005), p.1398.

[4] S. Suresh: Metall Trans, Vol. 14a (1983), p. 2375.

[5] A. Akhmad Korda, Y. Mutoh, Y. Miyashita, T. Sadasue, S.L. Mannan: Scripta Materialia. Vol. 54, no. 11, (2006), p.1835

[6] A. Sugeta, Y. Uematsu, E.I. Kuronaga, M. Jono: Journal of the Society of Materials Science, Japan, Vol. 54, no. 12, (2005), p. 1268.

[7] J.K. Shang, J.L. Tzou and R.O. Ritchie: Metall. Trans. A, Vol. 18A, (1987), p.1613.

[8] G. Chai and J. Pokluda: *In: "Fatigue 06",* Ed. W. S. Johnson, Elsevier, Atlanta, Georgia, USA, p. 0205A_06.

[9] R. Lillbacka, G. Chai, M. Ekh, P. Liu, E. Johnson, K. Runesson: Acta Materialia, Vol. 55 (2007), p. 5359.